SolarPACES 2023, 29th International Conference on Concentrating Solar Power, Thermal, and Chemical Energy Systems

Thermal Energy Storage Materials, Media, and Systems

https://doi.org/10.52825/solarpaces.v2i.755

Published: 18 Jul. 2025

Heat Transfer and Pressure Drop in Packed Beds of Crushed Rock Particles

Jaap Hoffmann[1,*] and Eduard Fourie[1]

[1]Stellenbosch University, South Africa

[*]Correspondence: Jaap Hoffmann, hoffmaj@sun.ac.za

Abstract. Thermal energy storage using packed beds of crushed rocks finds application in solar thermal power generation, building thermal comfort, and greenhouse climate control. Crushed rock particles are irregular in shape and size, but notwithstanding have a clearly discerning long, intermediate, and short axis. Consequently, particles tend to pack down with their short axis facing upwards. As a result, the flow resistance and heat transfer characteristics in a packed bed depend on the flow direction relative to particle orientation. For small applications, the flow through a packed bed is typically one-dimensional, and one may rely on empirical correlations for design purposes. In this work, we propose that tortuosity is included in the heat transfer and pressure drop correlations. We derived our correlations from a combination of discrete element modeling (DEM) and computational fluid dynamics (CFD) and verified our results experimentally.

Keywords: Packed Bed, Crushed Rocks, Thermal Energy Storage

1. Introduction

Thermal energy storage (TES) using packed beds of crushed rocks finds application in concentrated solar thermal power plants, process heat, building thermal comfort, and greenhouse climate control systems. Kröger [1] proposed the SunSPOT cycle, an asynchronous combined cycle comprising a solarized gas turbine cycle coupled to a steam turbine cycle. Waste heat from the gas turbine is stored in a rock bed TES for use after sunset. The efficiency of the combined cycle approaches that of a conventional molten salt system [2 Heller & Hoffmann]. However, utility-scale high-temperature solar receivers capable of delivering air at 1 200 °C to the gas turbine are currently at low technology readiness levels [3 Avila-Marin]. Heller and Gauché [4] proposed a direct storage charging cycle capable of boosting the temperature of the rock bed to ensure high thermal efficiency for the steam turbine. Allen [5] suggested that the cost of a rock bed TES system will be 15 – 23 times lower than that of the equivalent molten salt TES. He estimated that the size of a rock bed thermal energy storage facility using rocks with a spherical equivalent diameter of 20 mm for a 50 MW_e solar thermal power station would be 7 m deep and require a footprint of about 62 m × 62 m (see figure 1).

Crushed rock particles are characterized by size and shape. For size, the most popular descriptor is the diameter of the volume-equivalent sphere [Waddell, 1933, 6]. Barrett [7] proposed that shape is described by overall form, roundness, angularity, and surface texture (roughness). The overall form of a particle is described by the ratio between the measurement of two orthogonal axes and may be described in terms of aspect ratio or its derivatives, elongation, and flatness. Roundness has different definitions [6]; in this work, we assume roundness to be a measure of the overall convexity of the particle. We consider the number and sharpness of corners as descriptors of angularity. Sphericity is a combination of shape, roundness, and angularity. It refers to the ratio of the surface areas of the volume-equivalent spherical particle and the particle itself. Using 3D scanning technology, the volume, bounding box, and surface area of an irregular particle can be measured. From these, one can extract the volume equivalent spherical diameter, aspect ratio, and sphericity of the particle. Hoffmann [8] has shown that both particle size and sphericity occur naturally in the heat transfer equations for a packed bed.

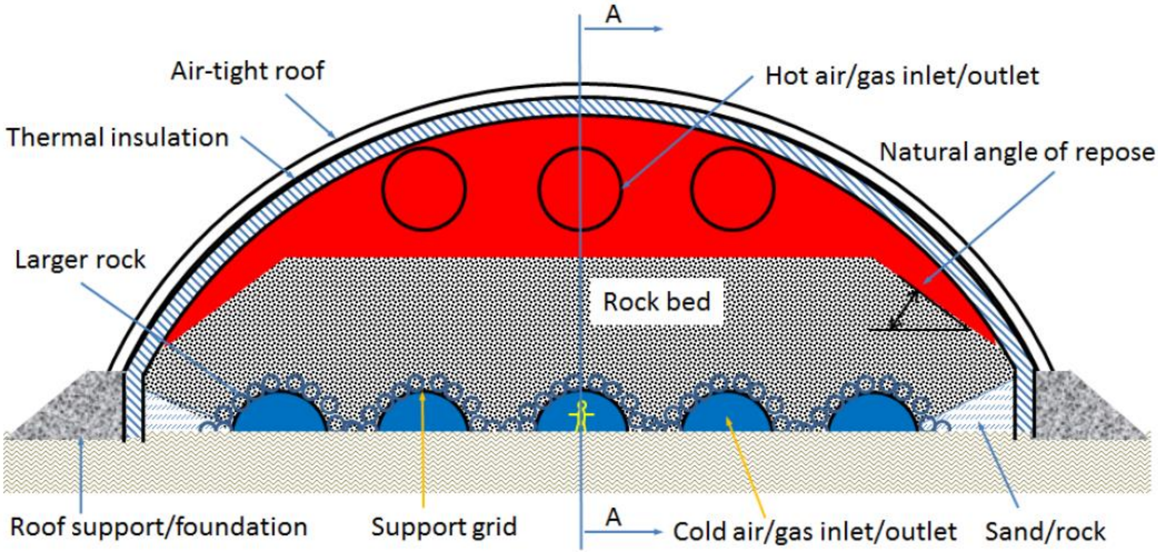

Figure 1. *Cross section through rock bed proposed by Allen [5].*

Crushed rock particles are irregular in shape and size, but notwithstanding have a clearly discerning long, intermediate, and short axis. Consequently, particles tend to pack down with their short axis facing upwards, as suggested in figure 3 (right). As a result, the flow resistance and heat transfer characteristics in a packed bed depend on the flow direction relative to particle orientation, as confirmed by Allen's [5] experimental results. Aspect ratio is the only one of the particle characteristics that contain directional information that may explain the behavior observed by Allen. Size distribution will affect packing density [9], but in this work, we deal with graded particles (passing a 75 mm sieve but retained on a 53 mm sieve), and we assume that the size distribution is narrow enough to adopt a bed of monodisperse particle sizes. Rolland et al. [2019, 10] have shown that the bed's void fraction is at least partially dependent on the particle shape. However, Du Toit and Rousseau [2014, 11] found that the pressure drop across a structured bed of spherical particles is a factor of two lower than that for an unstructured bed of identical particles with the same porosity.

For small applications, packed beds are typically confined in a prismatic container and the flow through the bed is one-dimensional, and one may rely on Ergun-like [12] correlations that correlate pressure drop against particle equivalent diameter and void fraction only for design purposes. Eisfeld and Schnitzlein [13] recognized that the pressure loss coefficient for flow through a packed bed also depends on the flow Reynolds number and the particle's specific surface area. The latter can be expressed in terms of sphericity if the characteristic size of the particle is taken as the diameter of its volume-equivalent sphere. Note that in Eisfeld and Schnitzlein's paper, the surface area equivalent sphere is used. However, the focus of Eisfeld and Schnitzlein's paper is on wall effects in small, prismatic reactors packed with spheres. Several correlations for the particle heat transfer coefficient, corrected for void fraction, are available from the literature [5]. Martin [14] has found an analogy between the friction factor and heat transfer, an approach that will be followed in this work. Most researchers [5] follow an approach suggested by Schuman that is based upon plug flow, a small Biot number for the particles, and assuming that the thermal capacity of the air is negligible compared to that of the rocks. Schuman's approach is computationally expedient, but for free-standing beds, the assumption of plug flow is invalid. Furthermore, the assumption of small Biot number breaks down for particle sizes greater than 10 mm. Allen [5] states that Schuman's model gives reasonable results for the average bed (rock) temperature for Biot numbers up to 0.2 (26 mm crushed rock particles).

In this work, we concentrate on utility-scale TES applications. Due to its large size, the packed bed will have multiple flow inlets and outlets, and three-dimensional flow patterns are expected. We derived our correlations from a combination of discrete element modeling (DEM) and computational fluid dynamics (CFD) and verified our results experimentally, and we propose that tortuosity is included in the heat transfer and pressure drop correlations.

2. Method

We collected data from 350 particles from crushed dolerite rock that passed through a 75 mm sieve but was retained on a 53 mm sieve. Most of the particles had a spherical equivalent diameter in the range of 30 mm – 70 mm, with a peak close to the mean particle diameter of 53.3 mm, as shown in Figure 2. The ellipsoids and bricks have the same volume, aspect ratio, and spherical equivalent diameter as the averages for crushed rocks, as shown in Table 1. Ellipsoids have a higher sphericity than the crushed rock particles, whilst that of the bricks is lower. In contrast, the roundness of both particles is lower than that of the crushed rock particles, but that of the ellipsoids is closer to that of the crushed rock particles than the bricks. Spherical particles lack direction information and were discarded in this study. There is little to choose between bricks and ellipsoids, and we selected an ellipsoid as our representative particle based on a recommendation by Li et al [15]. For the experiments, we made about 6 000 cement castings of the ellipsoids.

Table 1. *Average measurements of rock sample and that of its representative sphere and ellipsoid.*

	L	I	S	Vol	D_{ve}	SA	Elong-ation	Flat-ness	ψ	ϕ
	[mm]	[mm]	[mm]	[mm^3]	[mm]	[mm^2]	-	-	-	-
Rocks	80.5	55.2	34.0	79188	53.3	11235	1.458	0.616	0.794	0.631
Spheres	53.3	53.3	53.3	79188	53.3	8 918	1.000	1.000	1.000	1.000
Bricks	64.9	44.5	27.4	79188	53.3	11776	1.458	0.616	0.757	0.329
Ellipsoids	80.5	55.2	34.0	79188	53.3	9 840	1.458	0.616	0.906	0.422

In the table, ψ is the sphericity of the particles, and ϕ is its Cox roundness. Elongation is defined as L/I and flatness as S/I, with L, I, and S the lengths of the long, intermediate, and short axes respectively.

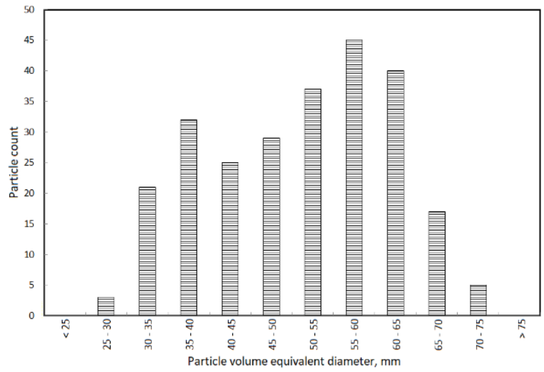

Figure 2. *Size distribution of crushed rock particles.*

2.1 Discrete element modelling

We used the Rocky DEM 2022R1 code to generate packed beds of ellipsoidal particles. The particles were dropped into a rigid spherical container with an opening at the top. The spherical shape allows us to change the flow direction through the bed by rotating the container in the elevation and azimuthal directions during our laboratory experiments. In subsequent computational fluid dynamics simulations of the flow and heat transfer in the voids, a rectangular domain was rotated to correspond to the same flow directions. The container vibrated at an amplitude of 10 mm and a frequency of 10 Hz during filling to ensure a close packing of particles. The container was allowed to overflow to give the particles time to settle in their final positions. The set-up and calibration of our DEM model are described in [16].

From the DEM model, information on the porosity and structure of the particles in the bed can be extracted, as shown in Figure 3. A wall-affected zone extends for about two particle diameters from the wall (Figure 3a), whilst Figure 3b shows the effect of the wall on particle orientation. The bulk porosity of the bed (38 - 42 %) agrees reasonably well with our experimental values (41 %). Repeating the DEM simulation four times using different particle release points (hopper positions) above the bed results in a 5 % fluctuation in the mean.

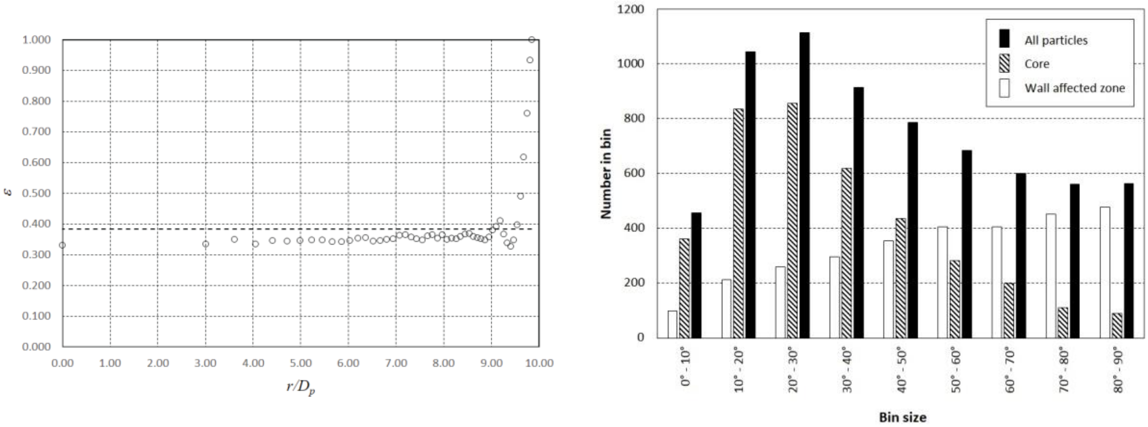

Figure 3. *Porosity distribution (left) and particle orientation (right) in the DEM-generated packed bed.*

2.2 Computational fluid dynamics

The particle positions and orientations obtained from the DEM model [17] were exported to the ANSYS 2023 R1 CFD code [18], and the particles were subtracted from the fluid domain to allow us to model the flow through the interstitial volumes. We performed two sets of CFD simulations. The first set was for validation purposes only and included all the particles. In the second set, the wall-affected zone was removed to get a better representation of the behavior of a free-standing rock pile. The latter served as the basis for our pressure drop and heat transfer predictions and the flow direction were changed through 18° in both the elevation and azimuthal angle for a total of 21 flow directions.

For both sets, superficial velocity through the bed was varied by about an order of magnitude from Re_p = 600 to Re_p = 8 500 by doubling the inlet velocity between runs for six runs per flow direction. The properties of air were calculated using the National Institute of Standards and Technology's (NIST) real gas model, based on the REFPROP v9.1 [19] database. Above particle Reynolds number of 350, the flow in a porous medium tends to be fully turbulent [13], and we used the shear stress transport k-w turbulence model throughout. A constant heat flux was described at the particle walls, whilst the side walls of the domain were modeled as slip walls. A constant velocity boundary condition is described at the domain inlet and a pressure outlet boundary condition at the domain outlet. Details of the mesh and the mesh independence study are given in [16]. Mesh independence is reached at about 20 million polyhedral cells, and simulations run for about 12 hours on a 120 CPU Intel Xeon 2.6 GHz cluster.

2.3 Model validation

For validation purposes, we simulated the full bed. After the model has been validated, we removed the wall-affected region (the outer two layers of particles) to get results more suited to infinite beds.

For the experiments, we poured about 6 000 particles into an expanded metal spherical container. Our laboratory facilities limited us to a container-to-particle diameter ratio of 20. We inserted a stencil of 7 heated and instrumented aluminum particles in the center of the container. The pressure drop across the container, as well as the average particle temperatures, were recorded.

3. Results

Our experimental and CFD results for heat transfer from ellipsoidal particles are within 5 % of each other. Considering that the porosity and packing structure between two random packings will never match, we consider the CFD model validated. Figure 4 (left) below shows the friction factor [13] for vertical flow through the bed from our experimental and CFD work. A plot of the modified (it includes sphericity) Ergun equation is also shown. The figure also indicates that the friction factor for crushed rock particles is higher than that of ellipsoids. We proposed a correlation for the pressure drop in some of our earlier work [2].

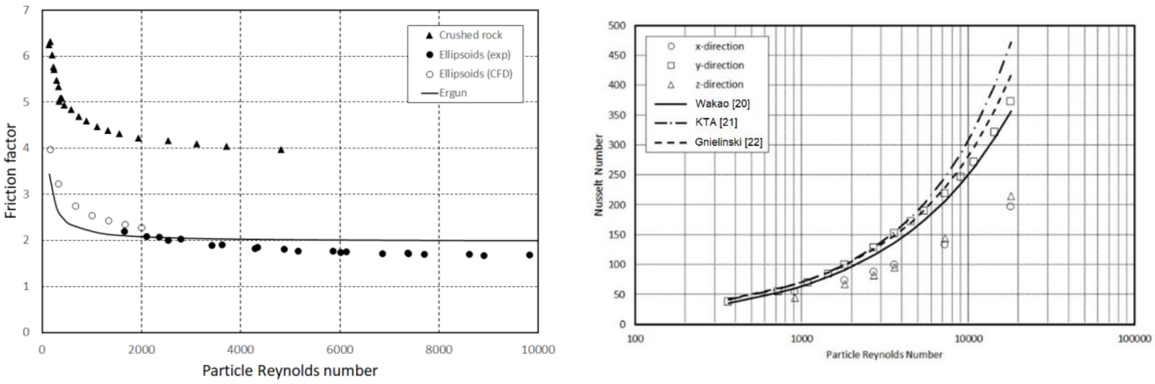

Figure 4. *Pressure drop (left) and Nusselt number for vertical flow through a packed bed of crushed rock compared to correlations for spherical particles.*

Figure 4 (right) shows a Nusselt number plot for vertical and horizontal flow through the bed. The Nusselt number for vertical flow is higher than that for horizontal flow and compares well with the literature. The Nusselt numbers for the two horizontal flow directions are similar.

From the CFD model, the hydraulic tortuosity is evaluated as [23]

$$\tau = \frac{\langle |u| \rangle}{\langle |u_t| \rangle} \tag{1}$$

With u_t the velocity component tangential to the main flow direction. This allowed us to formulate the Nusselt number in terms of tortuosity and superficial particle Reynolds number as

$$Nu = 0.2799\tau^{0.2981}Re^{0.8117}Pr^{0.3333} \tag{2}$$

Equation (2) fits our data within an average error of ± 9.8 %. The largest deviation between equation (2) and our data is 20.7 %.

We also compared our heat transfer data against the correlation of Martin [24], who evaluated experimental data for cubes, cylinders, rings, saddles, and spheres. Following the Lévêque analogy, Martin showed that the heat transfer coefficient depends on the pressure drop. Thus, his correlation can take the effect of flow orientation on the particle heat transfer coefficient into account. Our data follows the same trend as that of Martin but deviations at large Reynolds numbers are substantial, as shown in figure 5. We have started testing, but our current experimental data is limited to Re ~ 1 000.

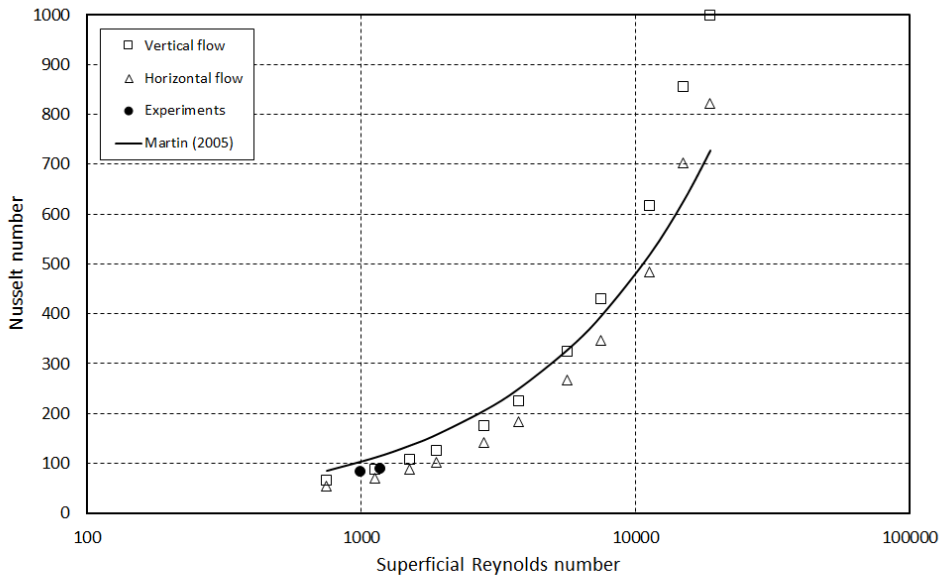

Figure 5. *Experimental and CFD data compared to Martin's [24] correlation.*

4. Conclusion

Our correlations are tailored for implementation in the commercial CFD code ANSYS Fluent and should be helpful in designing or evaluating pressure drop and heat transfer in utility-scale beds with multiple inlets and outlets, or smaller beds with baffles. There are still gaps between the data for ellipsoids and crushed rock particles that need to be resolved.

One can use the modeling results to design and optimize a hypothetical (Figure 6, left) or real packed bed. Using the CFD code ANSYS fluent, for example, the bed may be modeled as a porous zone, with inputs for heat transfer and pressure drop as shown in Figure 6 (right).

The coefficients on the main diagonal of the pressure drop tensor dominate, and the off-diagonal coefficients may be neglected in favor of the greater computational robustness it offers compared to entering the cross coefficients via user-defined functions. For superficial velocities greater than 0.04 m/s [16], the inertial term in the pressure drop equation exceeds the viscous term; at a mean superficial velocity of 0.233 m/s [5], the inertial term dominates, and the viscous term may be ignored.

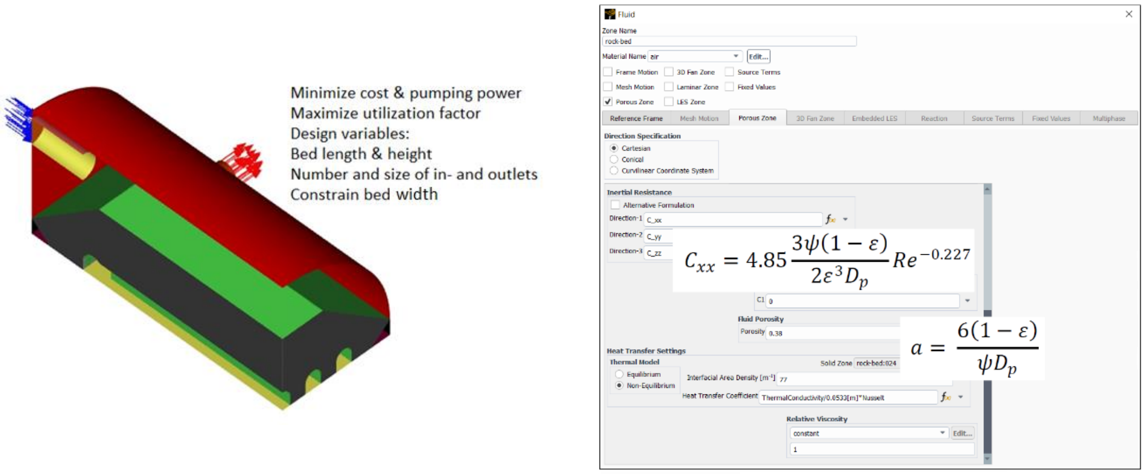

Figure 6. *Suggested use of anisotropic heat transfer and resistance models in packed bed simulation, design, and optimization.*

The heat transfer surface per unit volume is a function of particle diameter and sphericity, and the porosity of the bed. All three are usually known quantities. For the Nusselt number, equation (2) can be used, although tortuosity isn't necessarily known a priori. Efforts to predict tortuosity from the flow orientation relative to the global coordinate system are promising, but not conclusive. Validation of equation (2) and efforts to express tortuosity in terms of the flow direction are continuing.

Data availability statement

There is no relevant additional data to this article beyond the presented content.

Author contributions

Conceptualization, resources, supervision, writing and reviewing the paper - JH. Experimental validation and laboratory testing - EF.

Competing interests

The authors declare that they have no known competing financial interests or personal relationships that could have appeared to influence the work reported in this paper.

Funding

The work was funded by the Solar Thermal Energy Research Group.

Acknowledgment

The authors hereby acknowledge the Centre for High-Performance Computing (CHPC) South Africa, for providing computational resources to this research project.

References

[1] D.G. Kröger, (2011), The Stellenbosch University solar power thermodynamic cycle, https://sterg.sun.ac.za/wp-content/uploads/2011/05/SUNSPOT-2.pdf.

[2] L.J. Heller and J.E. Hoffmann, (2015), A cost and performance evaluation of SUNDISC: a dual-pressure air receiver cycle, Proceedings of SolarPACES 2014, Beijing, China, Energy Procedia, Vol. 69, 1287 – 1295.

[3] A.L. Avila-Marin, (2011), Volumetric receivers in solar thermal power plants with central receiver system technology: a review, Solar Energy, Vol. 85, pp. 891 – 911.

[4] L.J. Heller and P. Gauché, (2014), Dual-pressure air receiver cycle for direct storage charging, Proceedings of SolarPACES 2013, Las Vegas, USA, Energy Procedia, Vol. 49, pp. 1400 – 1409.

[5] K.G. Allen, (2014), Rock bed thermal storage for concentrating solar power plants, Ph.D. Thesis, Stellenbosch University.

[6] H. Wadell, (1933), Sphericity and roundness of rock particles, The Journal of Geology, Vol. 41, No. 3, pp. 310 – 331.

[7] P.J. Barret, (1980), The shape of rock particles: a critical review, Sedimentology, Vol. 27, pp. 291 – 303.

[8] J.E. Hoffmann, (2022), Determining the particle heat transfer coefficient for an anisotropic bed of crushed rock particles, Proceedings of HEFAT 2022, Amsterdam, The Netherlands.

[9] A. Dziugys, A.H. Mahmoudi, E. Misiulis, R. Navakas and G. Skarbalius, (2022), Fractal dependence of the packed bed porosity on the particles size distribution, Chaos, Solutions and Fractals, Vol. 159.

[10] M. Rolland, A.D. Rakotonirina, A. Devassoux, G.L.B. Goycetti, J.Y. Delenne and A. Wachs, (2019), Predicting average void fraction and void fraction uncertainty in fixed beds of poly lobed particles, Industrial & Engineering Chemistry Research, Vol. 58, pp. 3902 – 3911.

[11] C.G. du Toit and P.G. Rousseau, (2014), Separate effects tests to determine the pressure drop over packed beds in the PBMR HPTU test facility, Proceedings of HTR 2014, Weihai, China.

[12] S. Ergun, (1949), Fluid flow through packed columns, Chemical Engineering Progress, Vol. 48, pp. 89 – 94.

[13] B. Eisfeld and K. Schnitzlein, (2001), The influence of confining walls on the pressure drop in packed beds, Chemical Engineering Science, Vol. 56, pp. 4321 – 4329.

[14] H. Martin, (2005), The Lévêque-analogy or how to predict heat and mass transfer from fluid friction, Proceedings of HEFAT 2014, Cairo, Egypt.

[15] X. Li, M. Jiang, Z. Huang, and Q. Zhou, (2019), Effect of particle orientation on the drag force in random arrays of prolate ellipsoids in low Reynolds number flows, AIChE Journal, Vol. 65, pp. 1 – 11.

[16] E.B.E. Hassan and J.E. Hoffmann, (2023), A DEM-CFD Approach for Predicting Pressure Drop through Packed Bed of Crushed Rocks, Proceedings of SolarPACES 2022, Albuquerque, USA.

[17] ESSS Rocky, Release 2022 R2, User Manual, ESSS Rocky DEM, S.R.L., 2022.

[18] ANSYS Academic Research Fluent, Release 2023 R1, Help System, Solution Mode, ANSYS, Inc.

[19] Lemmon, E.W., Bell, I.H., Huber, M.L., McLinden, M.O., NIST Standard Reference Database 23: Reference Fluid Thermodynamic and Transport Properties-REFPROP, Version 9.1, National Institute of Standards and Technology, Standard Reference Data Program, Gaithersburg, 2018.

[20] Wakao, N., Kaguei, S., and Funazkri, T., (1979), Effect of fluid dispersion coefficients on particle-to-fluid heat transfer coefficients in packed beds, Chemical Engineering Science, Vol. 34, pp. 325 – 336.

[21] Safety Standards of the Nuclear Safety Standards Commission (KTA): KTA Rule 3102.3: Reactor Core Design of High-Temperature Gas-Cooled Reactors; Part 3: Loss of Pressure through Friction in Pebble Bed Cores, (March 1981).

[22] Gnielinski V., Fluid-particle heat transfer in flow through packed beds of solids, chapter G9 in VDI Wärmeatlas, 2nd edition, Springer, Düsseldorf, (2010).

[23] Fu, J., Thomas, H.R. and Li, C., (2021), Tortuosity of Porous Media: Image Analysis and Physical Simulation, Earth-Science Reviews, Vol. 212, https://doi.org/10.1016/j.earscirev.2020.103439

[24] Martin, H., (2005), The Lévêque Analogy, or How to Predict Heat and Mass Transfer from Fluid Friction, Proceedings of HEFAT 2005, Cairo, Egypt.